Proceedings of 2017 IEEE
International Conference on Mechatronics and Automation
August 6 - 9, Takamatsu, Japan

Design and Analysis of a Novel Lightweight Underwater Manipulator*

Chong Tang
Institute of Automation
Chinese Academy of Sciences;
University of Chinese Academy of Sciences
Beijing, China
tangchong2014@ia.ac.cn

Yu Wang*, Shuo Wang, Rui Wang, and Min Tan
Institute of Automation
Chinese Academy of Sciences
Beijing, China
{yu.wang,shuo.wang,rwang5212,min.tan}@ia.ac.cn

***Abstract*— This paper addresses the mechanism design of a novel lightweight underwater manipulator. This underwater manipulator has the properties of light weight, small size and uniform mass distribution. Specifically, the implement of every joint and the gripper of the underwater manipulator is presented. Then the forward kinematics model is built based on Denavit−Hartenberg principle, and the inverse differential kinematics model is established by virtue of Jacobian relationship. Moreover, the forward and backward recursive dynamics propagation model is introduced with consideration of hydrodynamics. Finally the simulation is conducted to verify the practicability of the underwater manipulator.**

***Index Terms*— Lightweight underwater manipulator, underwater gripper, underwater manipulation.**

I. Introduction

An underwater manipulator plays an important role in underwater rescue, equipment assembly, and environment protection. Therefore, the research on the underwater manipulator has drawn increasing attention. Jin et al. designed an underwater four-bar linkage mechanism manipulator for capturing starfish, which could be installed on the AUV [1]. Furthermore, the modeling, optimization, and experimental validation of the manipulator were given. Ishitsuka et al. devised a 2-link underwater manipulator and gave its kinematics, dynamics and RAC control method [2]. Lee et al. gave the design of a 5 degrees of freedom (DOF) manipulator for removing some particles at the bottom of a nuclear reactor vessel and a reactor coolant system, and the use of this manipulator contributed to improve the reliability of the nuclear reactor vessel [3]. Yao et al. developed a 7-function Hydraulic underwater manipulator as a slave arm. This arm was operated by a master arm installed on the master controller [4]. Additionally, Cobos-Guzman et al. presented a 3-DOF robotic arm for underwater tasks, and its design and modelling were elaborated [5]. Khan et al. gave the design of a 6-DOF underwater robotic manipulator with shoulder, elbow and wrist [6]. It was based on the principle of human hand. And its workspace was deduced.

In the design of these above manipulators, the motors are installed in their respective joints. Once the robot is equipped with these manipulators, the large reaction of the manipulator during its motion needs to be overcame. Consequently, a new lightweight manipulator was designed [7], which was covered with foam material to ensure light weight in water. It has been integrated in an AUV, and the free-floating manipulation has been achieved [8]–[12]. However, high arm velocities would result in the amplified the coupling between the manipulator and the robot. Therefore, a novel 4-DOF manipulator with a lightweight multi-link structure was developed in our previous work [13]. Since motors were placed inside the waterproof base installed on the vehicle, the waterproof base occupied most of the underwater manipulator's mass. This novel design could reduce the coupling between the manipulator and the vehicle. Finally, its free-floating autonomous manipulation at a relative high speed was implemented.

Based on the developed 4-DOF manipulator, this paper presents a 5-DOF manipulator, which can be installed on the underwater robot to achieve its floating manipulation. Compared with the developed manipulator in [13], wrist pitch joint is added in the new manipulator design, and the gripper is improved significantly. Moreover, the wrist pitch joint angle, roll joint and the gripper are driven by double wire ropes instead of single wire rope connected to a single motor respectively. This would ensure high joint control precision in reciprocating motion of every joint. Furthermore, the kinematics and dynamics of the manipulator are modeled to verify the feasibility of this manipulator.

The rest of the paper is organized as follows. The mechanism design of the lightweight manipulator is detailed in Section II. In Section III, the kinematics model and inverse differential model is built. While the dynamics model is introduced in Section IV. In Section V, simulations and results are given. Finally, conclusion and future work are summarized in Section VI.

*This work is supported in part by the National Natural Science Foundation of China under Grants #61233014, #61333016 to S. Wang, in part by the Foundation for Innovative Research Groups of the National Natural Science Foundation of China under Grant #61421004 to M. Tan, and in part by the Beijing Municipal Commission of Science and Technology under Grant #Z171100000817009 to S. Wang

II. Design of the Light Weight Manipulator

In this section, the mechanical design of the novel lightweight underwater manipulator with 5-DOF is elaborated. With our best knowledge, the underwater manipulator to be mounted on an underwater vehicle had better have light weight, small size, and uniform mass distribution. These will contribute to the reduction of the mass ratio between the manipulator and the vehicle body, and the improvement of stability of the underwater vehicle during performing manipulation. So the design in this paper is to pursue the achievement of those advantages.

A. Overview of the manipulator

The mechanism structure of the manipulator is illustrated in Fig. 1. This is a highly modularized underwater manipulator, which only needs the exterior power supplement and bidirectional information transmission with onboard processor. All motors and electronic equipments are placed in the waterproof base uniformly, as shown in Fig.1(c). Thus the rotation of the waterproof base would not induce obvious shift of the centre-of-gravity of the vehicle. This manipulator has 5 degree of freedom, i.e., waist roll joint, shoulder pitch joint, elbow pitch joint, wrist pitch joint, wrist roll joint, respectively. The gripper has two fingers with multiple knuckles, which can be used to grasp for various objects with different shapes and volumes effectively. In order to reduce the weight of the manipulator, the waist, shoulder and elbow joints are driven through gears, while the wrist pitch joint, wrist roll joint and the gripper are driven via bidirectional steel wire ropes.

As also shown in Fig. 1(a), the initial configuration is defined. The upper arm is vertical, while the forearm is horizonal. Their lengths are denoted as a_2 and a_3 respectively. When the gripper is naturally opened, the gripper length from the wrist pitch joint to the fingertip is denoted as d_5. Those selected parameters are inspired by the structure of the arm of the adult male. Next, the specific implementation of the mechanical structure of every joint will be detailed.

B. Implementation of the joints and gripper

The waterproof base (waist joint) is actuated by Servo Motor 1 via Reduction Gear 1, and rotates around the Fixed Gear. As shown in Fig. 1(c), the Reduction Gear 1 is connected to the Servo Motor 1. The Fixed Gear is fixed on the underneath of the underwater vehicle.

The upper arm (shoulder joint) is driven by Servo Motor 2, and the transmission is Worm and Reduction Gear 2. This worm-gear structure has the property of self-lock, i.e., the force can only be transmitted from the Worm to Reduction Gear 2 unidirectionally. This special design can avoid undesired outer disturbance.

The forearm (elbow joint) is actuated by Servo Motor 3. Elbow joint is far away from the the Servo Motor 3, so the transmission structure is more complex. As shown in Fig. 1(b) and Fig. 2, Reduction Gear 3 is connected to the shaft of the Servo Motor 3, and Reduction Gear 7 is connected to elbow

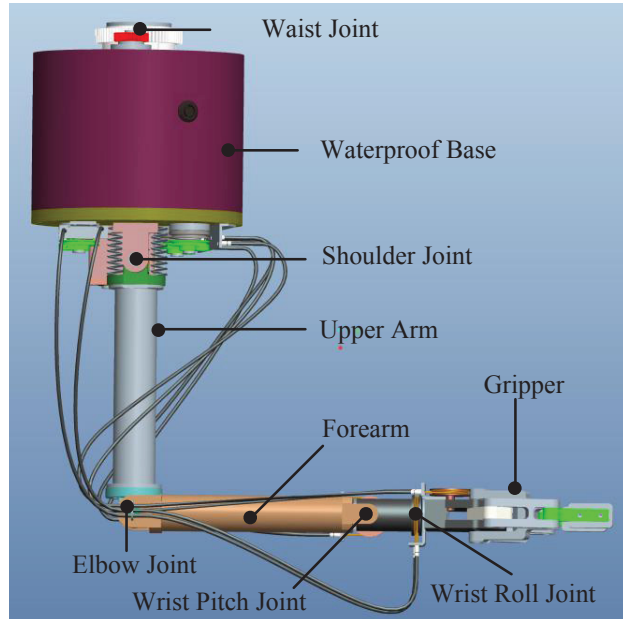

(a)

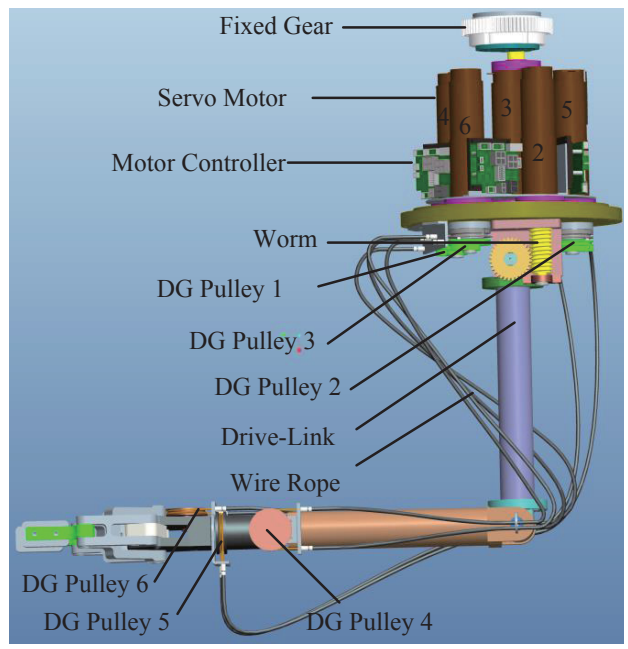

(b)

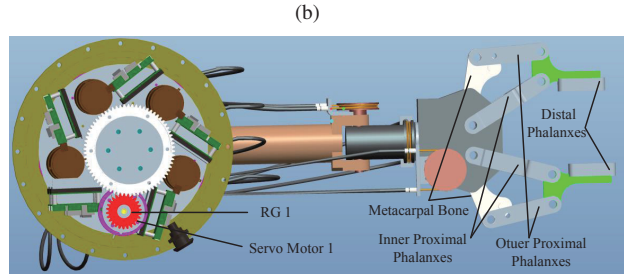

(c)

Fig. 1. Mechanism design of the manipulator. (a) Right view. (b) Left view. (c) Top view. RG and DG are the abbreviations of Reduction Gear and Double-Grooved respectively.

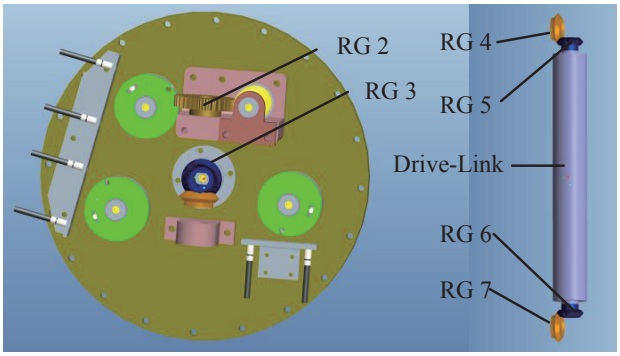

Fig. 2. Bottom view of the waterproof base and the drive link.

joint. The Reduction Gear 4-7 and Drive-Link play the role of bridge of drive.

Wrist joint can rotate in roll and pitch, i.e., wrist pitch joint and wrist roll joint. The wrist pitch joint and wrist roll joint are actuated by Servo Motor 4 and 5 respectively. They both are driven via double-grooved Pulley and double Wire Ropes. Wire Ropes are in tension all the time. So the wrist joint could be driven bidirectionally and precisely. Here reduction ratios are determined by the radii of capstan and driven double-grooved pulley.

The gripper is actuated by Servo Motor 6 via double-grooved Pulley and double Wire Ropes. As shown in Fig. 1(c), the gripper has two fingers. Every finger is composed of one metacarpal bone, one inner and one outer proximal phalanx and one distal phalanx. When the gripper performs the grasping mission, the inner proximal phalanxes and the distal phalanxes would touch the object fully. The open angle of the gripper is depended on the shape of the object and the rotational angles of Servo Motor 6.

III. Kinematics analysis and modeling

A. Establishment of reference frames

The initial position of the manipulator is depicted in Fig. 3. The upper arm sags naturally. The forearm lies in horizontal direction and points forward, so it is perpendicular to the upper arm. The gripper is opened naturally, and the plane formed by two fingers is also horizontal.

1) Base-fixed frame $O_0X_0Y_0Z_0$: The origin of the base-fixed frame O_0 is the point of intersection of rotation axis J_1 and J_2. Z_0 is along with J_1, and points downward. X_0 is parallel to the forearm, and points to the front. Y_0 is along with J_2, and the direction is determined by the right-handed coordinate principle.

2) Frame $O_1X_1Y_1Z_1$: The origin of the frame $O_1X_1Y_1Z_1$ coincides with X_0 exactly. Z_1 is along with J_2, and points outward. X_1 is parallel to X_0. Y_1 is along with J_1, and points upward.

3) Frame $O_2X_2Y_2Z_2$: The origin of the frame $O_2X_2Y_2Z_2$ is the point of intersection of upper arm and J_3. Z_2 is along with J_3, and points outward. X_2 has the same direction with $\overrightarrow{O_1O_2}$.

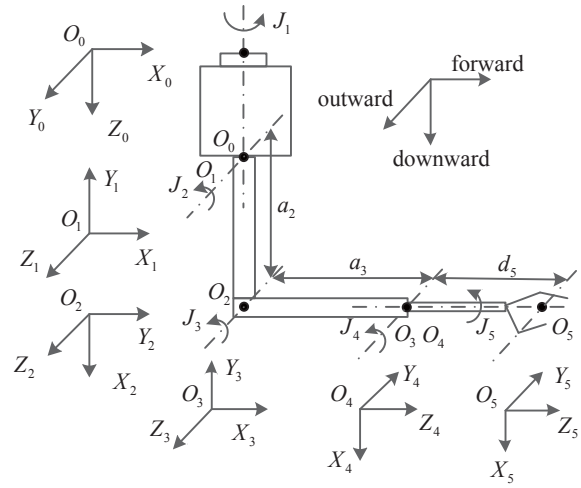

Fig. 3. Denavit−Hartenberg reference frames.

4) Frame $O_3X_3Y_3Z_3$: The origin of the frame $O_3X_3Y_3Z_3$ is the point of intersection of J_4 and J_5. Z_3 is along with J_4, and points outward. X_3 has the same direction with $\overrightarrow{O_2O_3}$.

5) Frame $O_4X_4Y_4Z_4$: The origin of the frame $O_4X_4Y_4Z_4$ coincides with X_3 exactly. Z_4 is along with J_5, and points to the front. X_4 points downward.

6) Frame $O_5X_5Y_5Z_5$: The origin of the frame $O_5X_5Y_5Z_5$ is the geometrical center of the gripper. Z_5 and Z_4 are collinear, and points to the front. X_5 is parallel to X_4.

Thus the established reference frames are shown in Fig.3.

B. Kinematics modeling

Since the reference frames have been established, the kinematics of the underwater manipulator can be deduced according to the relationship between two adjacent reference frames by Denavit−Hartenberg (DH) principle. The specific DH parameters are listed in Table I.

TABLE I
Denavit−Hartenberg Parameters

Link	$\theta(^\circ)$	d(mm)	a(mm)	$\alpha(^\circ)$
L_1	θ_1	0	0	-90
L_2	$\theta_2 - 90$	0	a_2	0
L_3	$\theta_3 + 90$	0	a_3	0
L_4	$\theta_4 - 90$	0	0	-90
L_5	θ_5	d_5	0	0

Hence the position and orientation of the end gripper with respect to $O_0X_0Y_0Z_0$ can be obtained by following coordinate transformation,

$$\begin{aligned} {}^0T_E &= \sum_{i=1}^{5} A_i \\ &= \begin{bmatrix} {}^0R_E & {}^0\eta_E \\ O_{1\times 3} & 1 \end{bmatrix}, \end{aligned} \tag{1}$$

where the ${}^0R_E \in R^{3\times3}$ and ${}^0\eta_E \in R^{3\times1}$ are the rotation matrix and position vector of the end gripper with respect to $O_0X_0Y_0Z_0$, respectively. $A_i, i = 1,2,3,4,5$ are the transformation matrices of the link frames, and they are able to be obtained by following equations.

$$A_1 = \begin{bmatrix} \cos\theta_1 & 0 & -\sin\theta_1 & 0 \\ \sin\theta_1 & 0 & \cos\theta_1 & 0 \\ 0 & -1 & 0 & 0 \\ 0 & 0 & 0 & 1 \end{bmatrix}. \tag{2}$$

$$A_2 = \begin{bmatrix} \sin\theta_2 & \cos\theta_2 & 0 & a_2\sin\theta_2 \\ -\cos\theta_2 & \sin\theta_2 & 0 & -a_2\cos\theta_2 \\ 0 & 0 & 1 & 0 \\ 0 & 0 & 0 & 1 \end{bmatrix}. \tag{3}$$

$$A_3 = \begin{bmatrix} -\sin\theta_3 & -\cos\theta_3 & 0 & -a_3\sin\theta_3 \\ \cos\theta_3 & -\sin\theta_3 & 0 & a_3\cos\theta_3 \\ 0 & 0 & 1 & 0 \\ 0 & 0 & 0 & 1 \end{bmatrix}. \tag{4}$$

$$A_4 = \begin{bmatrix} \sin\theta_4 & 0 & \cos\theta_4 & 0 \\ -\cos\theta_4 & 0 & \sin\theta_4 & 0 \\ 0 & -1 & 0 & 0 \\ 0 & 0 & 0 & 1 \end{bmatrix}. \tag{5}$$

$$A_5 = \begin{bmatrix} \cos\theta_5 & -\sin\theta_5 & 0 & 0 \\ \sin\theta_5 & \cos\theta_5 & 0 & 0 \\ 0 & 0 & 1 & d_5 \\ 0 & 0 & 0 & 1 \end{bmatrix}. \tag{6}$$

C. Inverse differential kinematics

In practice, the task to be performed is usually given in term of linear and angular velocity of the end-gripper. Differential kinematics is presented to describe the relationship between the joint velocities and the corresponding end-gripper linear and angular velocity.

The position and orientation of the end gripper with respect to $O_0X_0Y_0Z_0$ is completely determined by joint angles. So equation (1) can also be rewritten as

$$\eta_E = K(q), \tag{7}$$

where $\eta_E = [x, y, z, \psi, \theta, \phi]^T$ is the state vector of the end gripper, $q = [\theta_1 \ \ldots \ \theta_n]^T$ is the joint angle vector, and here $n = 5$. The differential relationship of Equation (7) is

$$\dot{\eta}_E = \dot{K}(q)\dot{q} = J(q)\dot{q}, \tag{8}$$

where $\dot{\eta}_E, \dot{q}$ are the time differential of the η_E, q respectively. $J(q) \in R^{6\times n}$ is the Jacobin matrix, and the Jacobin matrix can be obtained by

$$J(:,j) = [(z_{j-1} \times (p_E - p_{j-1}))^T, z_{j-1}^T]^T, \tag{9}$$

where the $J(:,j)$ is the $j-th$ column of J, z_{j-1}, p_{j-1} are the z-vector and position vector of frame $O_{j-1}X_{j-1}Y_{j-1}Z_{j-1}$ with $z_0 = [0,0,1]^T, p_0 = [0,0,0]^T$, and p_E is the position vector of the end-gripper.

Given the linear and angular velocity of the end-gripper, the joint velocities can be obtained by virtue of inverse differential kinematics,

$$\dot{q} = J^+(q)\dot{\eta}_E, \tag{10}$$

where $J^+ = J^T(JJ^T)^{-1}$ is the generalized inverse of the Jacobin matrix. If the manipulator posture q_0 is known, joint positions can be computed by integrating velocities over time. The integration can be performed in discrete time by resorting to numerical techniques, i.e.,

$$q(t_{k+1}) = q(t_k) + \dot{q}(t_k)\Delta t. \tag{11}$$

Nevertheless, the Jacobian matrix J may lose full rank, that will result in kinematic singularities. So a singular value oriented regulated kinematic singularity form is

$$J^+ = J^T(JJ^T + P(\Sigma(JJ^T)))^{-1}, \tag{12}$$

where $P(\Sigma(JJ^T))$ is the bell-shaped and positive matrix function, and Σ is computed by $JJ^T = U\Sigma V^T$. This function will prevent J^+ from growing to infinite, and avoid kinematic singularity.

IV. Dynamics analysis and modeling

The manipulator is assumed to be rigid bodies numbered from 1 to n, thus the manipulator is regarded as an open kinematic chain, and a recursive dynamics model can be established based on the reference frames.

The forward recursive propagation can be written as

$${}^{i+1}\upsilon_{i+1} = {}^i T_{i+1}^T \, {}^i\upsilon_i + \dot{q}_{i+1}z, \tag{13}$$

where ${}^i\upsilon_i \in R^6$ is the vector of linear and angular velocity of frame i, and $z = [0,0,0,0,0,1]^T$ for the rotational joint. ${}^iT_{i+1} \in R^{6\times6}$ is defined as

$${}^iT_{i+1} = \begin{bmatrix} {}^iR_{i+1} & O_{3\times3} \\ S({}^iP_{i,i+1}){}^iR_{i+1} & {}^iR_{i+1} \end{bmatrix}, \tag{14}$$

where $S(\cdot)$ is the cross product operator, and the ${}^iP_{i,i+1}$ is the vector from frame i to $i+1$ expressed in frame i.

Here, the velocity of gravity center of link $i+1$ can also be computed by the above propagation equation analogously,

$${}^{i+1}\upsilon_{i+1,c} = {}^i T_{i+1,c}^T \, {}^i\upsilon_i + \dot{q}_{i+1}z, \tag{15}$$

where ${}^iP_{i,i+1}$ is substituted by ${}^iP_{i,i+1,c}$ in matrix ${}^iT_{i+1,c}$.

Define ${}^i\tau_{i,l}$ as the generalized force of link i, and ${}^i\tau_i$ as the total generalized force acting on the link i. The backward recursive propagation can be expressed as

$${}^i\tau_i = {}^i T_{i+1} \, {}^{i+1}\tau_{i+1} + {}^i\tau_{i,l}, \tag{16}$$

where ${}^n\tau_n$ is the interaction force with intervention object, and the ${}^i\tau_{i,l}$ can be described by following dynamics equation of link i,

$$M_i \, {}^i\dot{\upsilon}_{i,c} + C_i \, {}^i\upsilon_{i,c} + D_i \, {}^i\upsilon_{i,c} + G_i(R_i) = {}^i\tau_{i,l}, \tag{17}$$

where M_i, C_i, D_i, G_i are all time varying coefficients. M_i is the inertia matrix including added mass effects. $C_i = C_i({}^i\upsilon_{i,c}, M_i)$ is the matrix of Coriolis and centripetal terms

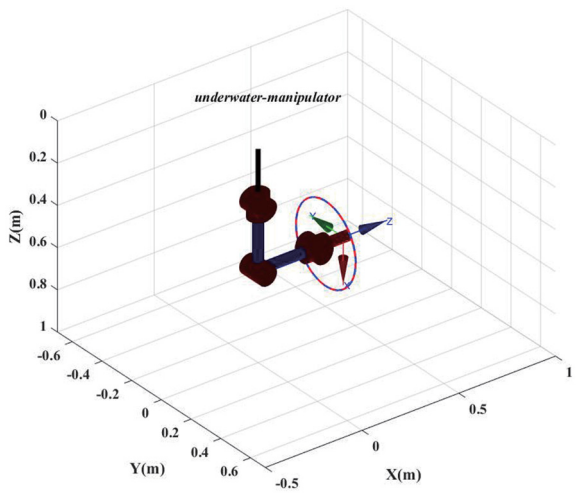

Fig. 4. The simulation model of the manipulator.

including added mass effects and hydrodynamics, and it is determined by velocity of center of gravity ${}^{i}\upsilon_{i,c}$ and inertia matrix M_i. $D_i = D_i({}^{i}\upsilon_{i,c}, \rho, C_d, d)$ is the matrix of friction and hydrodynamic damping term, decided by the velocity of center of gravity ${}^{i}\upsilon_{i,c}$, medium density ρ, hydrodynamic damping coefficient C_d and link diameter d. The last term $G_i(R_i)$ is the vector of gravitational and buoyant forces.

So the needed torque of every joint of the underwater manipulator can be obtained by

$$\tau_{q,i} = z^T \, {}^{i}\tau_i, \tag{18}$$

where $\tau_{q,i}$ is the moment the servo motor needs to provided.

V. Simulations and Results

In practical applications, the computation of inverse kinematics is much more sophisticated than the inverse differential kinematics. Especially, when the singularity point is reached, it's hard to calculate the inverse kinematics. In this section, the end gripper will draw a circle in two laps based on the forward kinematics and inverse differential kinematics. This is a simulation of turning a valve continuously in underwater environment. The center of the circle is located at $[0.35, 0, 0.56]^T m$, and the radius of the circle is $0.2m$. The circle lies in YZ plane, and the angle velocity is $[\pi/15, 0, 0]^T rad/s$.

The simulation model of the manipulator is depicted in Fig.4. The blue solid circle is the desired circle, and the red dash circle is the actual trajectory of the end gripper. From Fig.4, we can find that the red dash circle and blue solid circle are overlapped well. The norm error is illustrated in Fig.5. The error changes periodically and the peak errors occur at the opposite points of the initial position.

The desired velocities are shown in Fig. 6. The velocity in X direction is zero due to that the circle is in YZ plane. Those desired velocities are transformed from the task operational space to joint space by virtue of the corresponding Jacobian relationship. Fig. 7 describes the trajectories of all joints. Those joint angles make the manipulator realize the desired circle

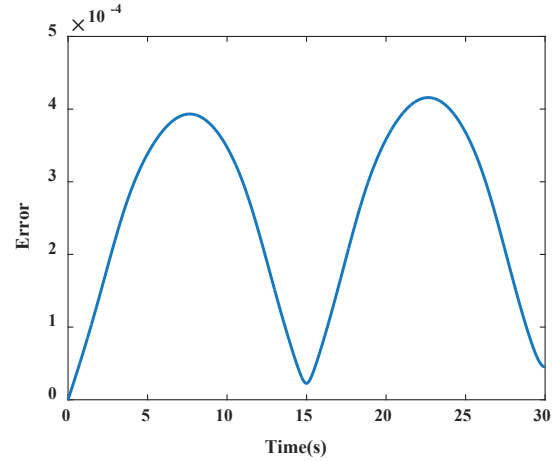

Fig. 5. The norm-2 error between the desired circle and actual circle.

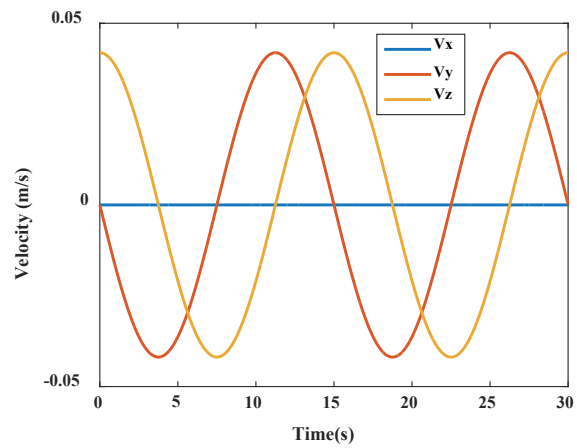

Fig. 6. Desired velocities.

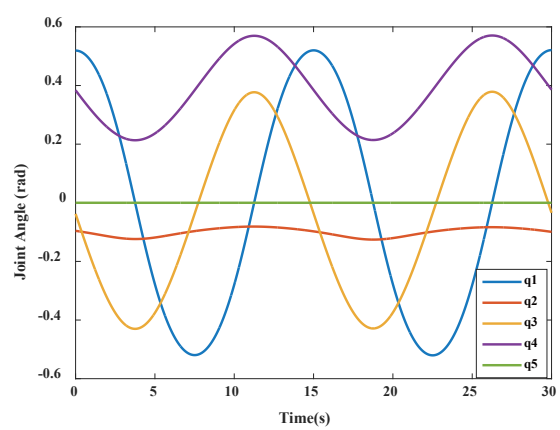

Fig. 7. Joint angle of the manipulator.

trajectory. But note that the solution of the joint angle is not unique due to the underdetermined equations in this system. Moreover, the manipulability of the manipulator is evaluated during the manipulator drawing the circle. As shown in Fig. 8,

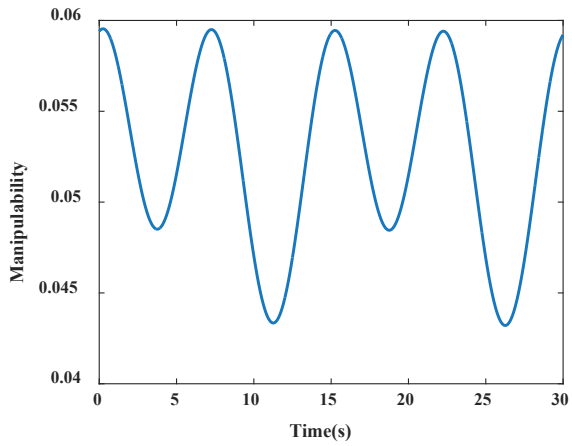

Fig. 8. The manipulability of the manipulator.

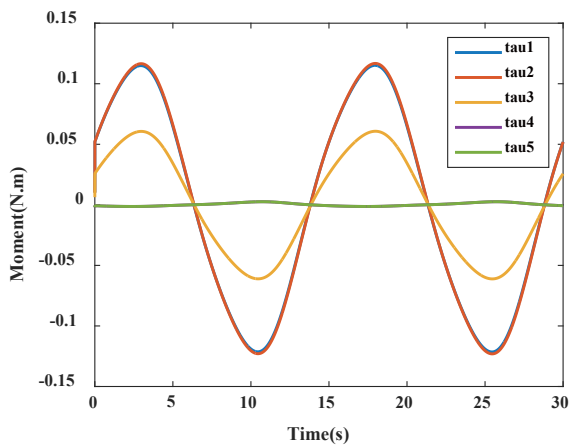

Fig. 9. The moment of every joint.

the manipulability of the manipulator is always positive, i.e., there is no singularity during this process. If the manipulability is closed to zero, robust calculation method has to be adopted.

In this simulation, suppose that the manipulator is installed on a fixed base, thus only the moment of joints of the manipulator need to be computed. Here the interaction force between the gripper and the intervention object is assumed to be linear associated to the tuning velocity. The needed moment of every joint is illustrated in Fig. 9. The servo motors provides the moment for the manipulator.

VI. Conclusions and Futures Works

In this paper, the mechanical design of a novel lightweight underwater manipulator has been detailed. The implement of every joint and the gripper of the underwater manipulator were reported. The forward kinematics model and inverse differential kinematics model were built respectively. The forward and backward dynamics models of the manipulator were also built. A simulation has also been carried out, and this simulation was the basic premise for turning a valve. The simulation results have proven that the underwater manipulator is of practicability.

In the future, the manipulator will be developed and constructed, and further installed on the underwater vehicle to perform underwater manipulation missions.

References

[1] S. Jin, J. Kim, J. Bae, T. Seo, and J. Kim, "Design, modeling and optimization of an underwater manipulator with four-bar mechanism and compliant linkage," *Journal of Mechanical Science and Technology*, vol. 30, no. 9, pp. 4337–4343, 2016.

[2] M. Ishitsuka, and K. Ishii, "Development of an underwater manipulator mounted for an AUV," in *Proceedings of MTS/IEEE OCEANS*, 2005, pp. 1811–1816.

[3] S. U. Lee, Y. S. Choi, K. M. Jeong, and S. Jung, "Development of an underwater manipulator for maintaining nuclear power reactor," in *Proceedings of IEEE International Conference on Control, Automation and Systems*, COEX, Seoul, Korea, 2007, pp. 1006–1010.

[4] J. Yao, L. Wang, P. Jia, and Z. Wang, "Development of a 7-function hydraulic underwater manipulator system," in *Proceedings of IEEE International Conference on Mechatronics and Automation*, Changchun, China, 2009, pp. 1202–1206.

[5] S. Cobos-Guzman, J. Torres, R. Lozano, T. Seo, and J. Kim, "Design of an underwater robot manipulator for a telerobotic system," *Robotica*, vol. 31, no. 6, pp. 945–953, 2013.

[6] A. Khan, and W. L. Quan, "Structure design and workspace calculation of 6-DOF underwater manipulator," in *Proceedings of 14th International Bhurban Conference on Applied Sciences and Technology*, Islamabad, Pakistan, 2017, pp. 651–655.

[7] J. J. Fernandez, M. Prats, P. J. Sanz, J. C. Garcia, R. Marin, M. Robinson, D. Ribas, and P. Ridao, Grasping for the seabed: developing a new underwater robot arm for shallow-water intervention, *IEEE Robotics and Automation Magazine*, vol. 20, no. 4, pp. 121–130, 2013.

[8] P. Cieslak, P. Ridao, and M. Giergiel, "Autonomous underwater panel operation by GIRONA500 UVMS: A practical approach to autonomous underwater manipulation," in *Proceedings of IEEE International Conference on Robotics and Automation*, Tokyo, Japan, 2015, pp. 529–536.

[9] D. Ribas, P. Ridao, A. Turetta, C. Melchiorri, G. Palli, J. J. Fernandez, P. J. Sanz, "I-AUV mechatronics integration for the TRIDENT FP7 project," *IEEE/ASME Transactions on Mechatronics*, vol. 20, no. 5, pp. 2583–2592, 2015.

[10] E. Simetti, G. Casalino, S. Torelli, A. Sperind, and A. Turetta, "Underwater floating manipulation for robotic interventions," in *Proceedings of 19th IFAC World Congress*, Cape Town, South Africa, 2014, pp. 3358–3363.

[11] R. Conti, F. Fanelli, E. Meli, A. Ridolfi, and R. Costanzi, "A free floating manipulation strategy for Autonomous Underwater Vehicles," *Robotics and Autonomous Systems*, vol. 87, no. 4, pp. 133–146, 2017.

[12] O. Kermorgant, Y. Petillot, and M. Dunnigan, "A global control scheme for free-floating vehicle-manipulators," in *Proceedings of IEEE/RSJ International Conference on Intelligent Robots and Systems*, Tokyo, Japan, 2013, pp. 5015–5020.

[13] Y. Wang, S. Wang, Q. Wei, M. Tan, C. Zhou, and J. Yu, "Development of an underwater manipulator and its free-floating autonomous operatio," *IEEE/ASME Transactions on Mechatronics*, vol. 21, no. 2, pp. 815–824, 2016.